

## Low-energy $E1$ strength in select nuclei: Possible constraints on neutron skin and symmetry energy

Tsunenori Inakura,<sup>1,2</sup> Takashi Nakatsukasa,<sup>2,3</sup> and Kazuhiro Yabana<sup>2,3</sup>

<sup>1</sup>*Department of Physics, Graduate School of Science, Chiba University, Yayoi-cho 1-33, Inage, Chiba 263-8522, Japan*

<sup>2</sup>*RIKEN Nishina Center, Wako 351-0198, Japan*

<sup>3</sup>*Center for Computational Sciences, University of Tsukuba, Tsukuba 305-8571, Japan*

(Received 14 June 2013; published 15 November 2013)

Correlations between low-lying electric dipole ( $E1$ ) strength and neutron-skin thickness are systematically investigated with a fully self-consistent random-phase approximation by using the Skyrme energy functionals. The presence of a strong correlation among these quantities is currently under dispute. We find that a strong correlation is present in properly selected nuclei, namely, in spherical neutron-rich nuclei in the region where the neutron Fermi levels are located at orbits with low orbital angular momenta. A significant correlation between the fraction of the energy-weighted sum value and the slope of the symmetry energy is also observed. A deformation in the ground state seems to weaken the correlation.

DOI: [10.1103/PhysRevC.88.051305](https://doi.org/10.1103/PhysRevC.88.051305)

PACS number(s): 21.10.Pc, 21.60.Jz, 25.20.-x

The isospin-dependent part of the nuclear equation of state, especially the symmetry energy, is receiving current attention. Although the symmetry energy at the saturation density  $E_{\text{sym}}(\rho_0)$  is relatively well known, its values at other densities, which have a strong impact on the description of neutron stars and stellar explosions, are poorly determined at present. Information on the density dependence of the symmetry energy might be obtained from the neutron-skin thickness  $\Delta r_{np}$  since the skin thickness was found to be strongly correlated with the slope  $L$  of the symmetry energy  $L = 3\rho_0 E'_{\text{sym}}(\rho_0)$  [1,2]. However, the large uncertainties in measured neutron-skin thickness have practically prohibited us from performing an accurate estimate on  $L$ .

The electric dipole ( $E1$ ) response is a fundamental tool for probing the isovector property of nuclei. The giant dipole resonance (GDR), which is rather insensitive to the structure of an individual nucleus, provides information on the magnitude of the symmetry energy near the saturation density  $\rho_0$ . In contrast, the low-energy  $E1$  modes, which are often referred to as pygmy dipole resonances (PDRs), are sensitive to the nuclear structure, such as the existence of loosely bound nucleons. Thus, the PDR, which is currently of significant interest in the physics of exotic nuclei, may carry information on the symmetry energy  $E_{\text{sym}}(\rho)$  at densities away from  $\rho_0$ .

Among many issues on the PDR, the correlation between the PDR and the neutron skin is one of the important subjects currently under dispute. If a strong correlation exists, the PDR may constrain both  $\Delta r_{np}$  and slope parameter  $L$ . The calculation by Piekarewicz with the random-phase approximation (RPA), based on the relativistic mean-field model, predicted a linear correlation for Sn isotopes [3]. By utilizing similar arguments, the neutron-skin thickness and the slope parameter were estimated from available data in  $^{208}\text{Pb}$ ,  $^{68}\text{Ni}$ ,  $^{132}\text{Sn}$ , and so on [4,5]. However, Reinhard and Nazarewicz performed a covariance analysis that investigated the parameter dependence for the Skyrme functional models, which concluded that the correlation between PDR strength and  $\Delta r_{np}$  is very weak [6]. Recently, they have extended their studies to the  $E1$  strength at finite momentum transfer  $q$  [7]. It should be noted that these conclusions, which seemed to

contradict to each other, were given from RPA calculations for specific spherical nuclei by using different methods of analysis.

Recently, we have performed a systematic RPA calculation on the PDR for even-even nuclei [8] by using the finite amplitude method [9–13]. The calculation is self-consistent with the Skyrme energy functional and fully takes into account the deformation effects. We found that a significant enhancement of the PDR strength takes place in regions of specific neutron numbers. The main purpose of the present Rapid Communication is to show that the quality of the correlation between PDR strength and  $\Delta r_{np}$  also is sensitive to the neutron number of the isotopes. Namely, a strong correlation exists only in particular neutron-rich nuclei. This may provide a possible suggestion for future measurements to constrain  $\Delta r_{np}$  and  $L$ .

*Numerical calculations.* We perform an analysis similar to Ref. [6] to investigate the Skyrme parameter dependence of the RPA results for nuclei of many kinds (mostly with  $Z \leq 40$ ), which include stable, neutron-rich, spherical, and deformed nuclei. The fully self-consistent RPA equation is solved by using a revised version of the RPA code in Ref. [14]. The size of the RPA matrix is reduced by assuming the reflection symmetry of the ground state with respect to  $x = 0$ ,  $y = 0$ , and  $z = 0$  planes. We adopt the representation of the three-dimensional adaptive Cartesian grids [15] within a sphere of the radius  $R_{\text{box}} = 15$  fm. The real-space representation has an advantage over other representations, such as the harmonic-oscillator basis, on the treatment of the continuum states. The Skyrme functional of the SkM\* parameter set [16] is used unless otherwise specified. The residual interaction in the present calculation contains all terms of the Skyrme interaction, which include the residual spin-orbit, the residual Coulomb, and the time-odd components. The pairing correlation is neglected for simplicity, which has little impact on  $E1$  modes [17].

*Definition of PDR strength, PDR fraction, and correlation coefficient.* We define the PDR strength as

$$S_{\text{PDR}} \equiv \int_0^{\omega_c} S(E1; E) dE = \sum_n^{E_n < \omega_c} B(E1; n), \quad (1)$$

with the PDR cutoff energy  $\omega_c$ . The PDR fraction  $f_{\text{PDR}}$  is the ratio of the integrated photoabsorption cross section below  $\omega_c$  to the total integrated cross section,

$$f_{\text{PDR}} = \frac{\int^{\omega_c} \sigma_{\text{abs}}(E) dE}{\int \sigma_{\text{abs}}(E) dE} = \frac{\sum_n^{E_n < \omega_c} E_n B(E1; n)}{\sum_n E_n B(E1; n)}. \quad (2)$$

In Eqs. (1) and (2), we fix the cutoff at  $\omega_c = 10$  MeV. Many former papers adopted the same definition [6,8] because of its simplicity. In light spherical neutron-rich nuclei, the value of  $\omega_c = 10$  MeV can reasonably separate the PDR peaks from the GDR. However, for heavier nuclei, the separation becomes more ambiguous. It is especially difficult for deformed nuclei. Later, we introduce another definition of the PDR strength by using a variable  $\omega_c$  to check the validity.

To quantify the correlation between two quantities, we use the correlation coefficient  $r$ . When we have data points for  $(x_i, y_i)$  with  $i = 1, \dots, N_d$ , it is defined by

$$r \equiv \frac{\sum_{i=1}^{N_d} (x_i - \bar{x})(y_i - \bar{y})}{\sqrt{\sum_{i=1}^{N_d} (x_i - \bar{x})^2} \sqrt{\sum_{j=1}^{N_d} (y_j - \bar{y})^2}}, \quad (3)$$

where  $\bar{x}$  and  $\bar{y}$  are the mean values of  $x_i$  and  $y_i$ , respectively. The absolute value of  $r$  does not exceed the unity. A perfect linear correlation,  $y_i = ax_i + b$ , corresponds to  $r = \pm 1$  with the same sign as that of parameter  $a$ . In the following, the correlation with  $r > 0$  ( $r < 0$ ) is referred to as ‘‘positive’’ (‘‘negative’’) correlation.

*Neutron-skin thickness in  $^{208}\text{Pb}$ .* First, we confirm the result in Ref. [6]. Reference [6] reported that the  $S_{\text{PDR}}$  for  $^{132}\text{Sn}$  only has a weak correlation with the neutron-skin thickness defined by  $\Delta r_{np} \equiv \sqrt{\langle r^2 \rangle_n} - \sqrt{\langle r^2 \rangle_p}$  of  $^{208}\text{Pb}$ . In Fig. 1, the  $S_{\text{PDR}}$  for  $^{132}\text{Sn}$  is shown as a function of the neutron-skin thickness  $\Delta r_{np}$  of  $^{208}\text{Pb}$ . The plotted 21 points are obtained by calculating  $\Delta r_{np}$

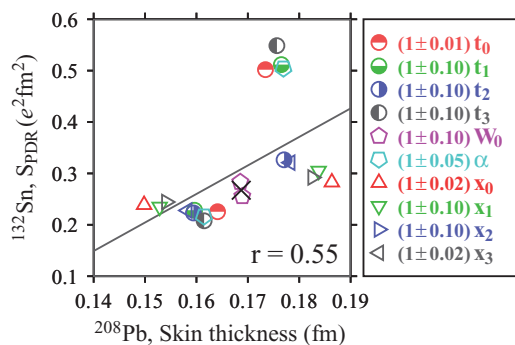


FIG. 1. (Color online) Correlations between the PDR strength  $S_{\text{PDR}}$  in  $^{132}\text{Sn}$  and the neutron-skin thickness  $\Delta r_{np}$  in  $^{208}\text{Pb}$ . The cross denotes a result obtained with the original SkM\* parameter set. Other symbols represent results with the modified parameter set as shown in the right panel. The solid line indicates a linear fit. The correlation coefficient for these parameter sets is also shown. See the text for details.

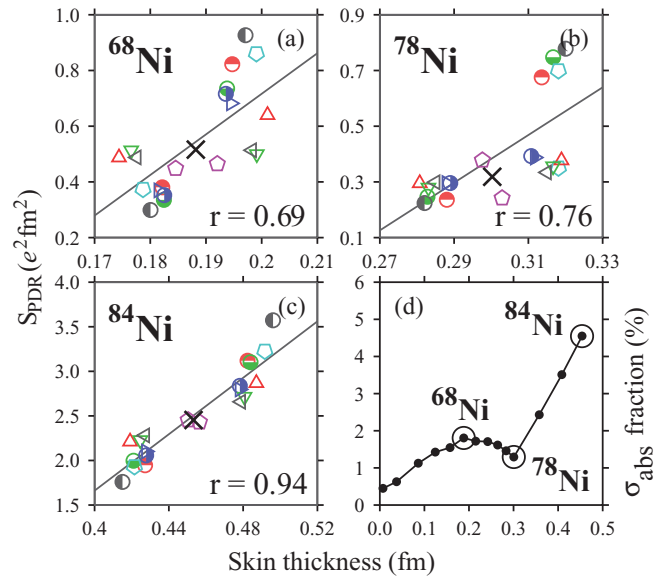


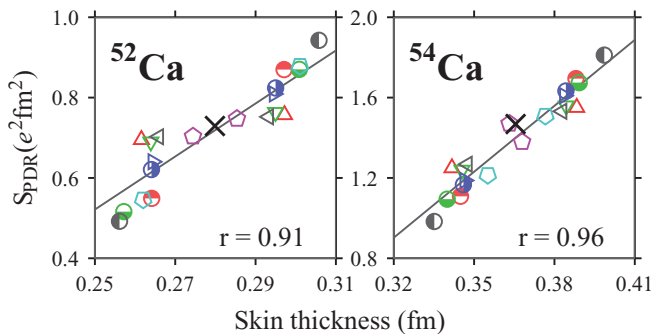
FIG. 2. (Color online) (a)–(c) Correlations between  $S_{\text{PDR}}$  and  $\Delta r_{np}$  in  $^{68,78,84}\text{Ni}$ . See the caption of Fig. 1. Calculated correlation coefficients are also shown. (d)  $f_{\text{PDR}}$  as functions of  $\Delta r_{np}$  for even-even Ni isotopes, calculated with the SkM\* parameter set. See the text for details.

and  $S_{\text{PDR}}$  with the SkM\* functional and with slightly modified values of 10 Skyrme parameters ( $t_{0,1,2,3}$ ,  $x_{0,1,2,3}$ ,  $W_0$ , and  $\alpha$ ). It seems to indicate some correlation, however, that the calculated points are somewhat scattered.

Using these 21 sample values ( $N_d = 21$ ), the correlation coefficient  $r$  is calculated according to Eq. (3). In the present case of Fig. 1, we obtain the coefficient  $r = 0.55$ . The correlations between  $\Delta r_{np}$  in  $^{208}\text{Pb}$  and  $S_{\text{PDR}}$  in  $^{68}\text{Ni}$  and  $^{78}\text{Ni}$  also are weak with  $r = 0.5$ – $0.6$ . Thus, the PDR strength in these spherical (magic) nuclei indicates a positive correlation with the skin thickness in  $^{208}\text{Pb}$ , however, the correlation is weak. This is qualitatively consistent with the result in Ref. [6].

*Correlation between  $S_{\text{PDR}}$  and  $\Delta r_{np}$ .* Next, we discuss the same correlation but between  $\Delta r_{np}$  and  $S_{\text{PDR}}$  in the same nucleus. In Fig. 2, we show the results for  $^{68}\text{Ni}$  ( $N = 40$ ),  $^{78}\text{Ni}$  ( $N = 50$ ), and  $^{84}\text{Ni}$  ( $N = 56$ ). The scattered data points in Fig. 2(a) suggest a relatively weak correlation in  $^{68}\text{Ni}$ , whereas, the correlation becomes moderately strong for  $^{78}\text{Ni}$ . The calculated correlation coefficients are  $r = 0.69$  and  $0.76$  for  $^{68,78}\text{Ni}$ , respectively. In contrast, a very strong linear correlation with  $r = 0.94$  for  $^{84}\text{Ni}$  is observed in Fig. 2(c). It is apparent that the linear correlation is qualitatively different among the isotopes.

The qualitative difference in  $S_{\text{PDR}}$  among the isotopes was previously observed in the PDR photoabsorption cross section [8]. In Ref. [8], we systematically calculated, for even-even nuclei up to  $Z = 40$ , the PDR fraction  $f_{\text{PDR}}$ . Then, we found that  $f_{\text{PDR}}$  significantly increases as a function of neutron number in regions where the neutron Fermi levels are located at the weakly bound low- $\ell$  shells, such as  $s$ ,  $p$ , and  $d$  orbits. In Ni isotopes, this corresponds to the region with a neutron number beyond 50 as illustrated in Fig. 2(d). Thus, the present result [Figs. 2(a)–2(c)] indicates that the neutron shell

FIG. 3. (Color online) Same as Fig. 2 but for  $^{52,54}\text{Ca}$ .

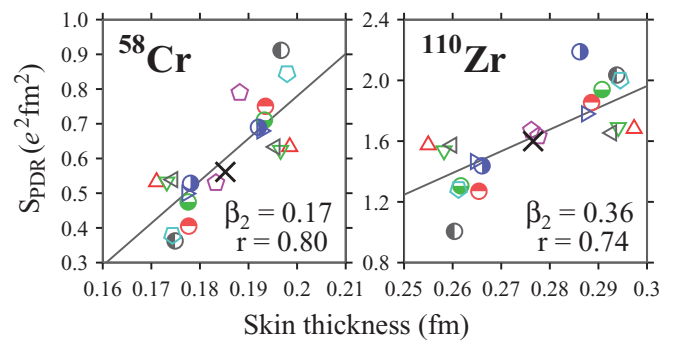
effect also has a significant impact on the linear correlation between the neutron-skin thickness and the PDR strength.

We confirm the same neutron shell effect in other light spherical isotopes;  $^A\text{O}$  and  $^A\text{Ca}$ . For Ca isotopes, the PDR strength appears beyond  $N = 28$  [8]. Accordingly, a strong linear correlation can be seen for  $^{52}\text{Ca}$  and  $^{54}\text{Ca}$  in Fig. 3. The calculated correlation coefficients are  $r = 0.91$  and  $0.96$  for  $^{52,54}\text{Ca}$ , respectively. These nuclei have more than 28 neutrons, and the neutron Fermi level is located at the  $p$  shell. They are predicted to have PDR peaks around  $E = 8$  MeV with  $f_{\text{PDR}} \approx 0.03\text{--}0.04$  [8]. In contrast, nuclei with  $N \leq 28$  have very small values of  $f_{\text{PDR}} < 0.01$ , and the linear correlation in  $^{48}\text{Ca}$  ( $N = 28$ ) indicates  $r = 0.78$ , which is much weaker than  $^{52,54}\text{Ca}$ . For O isotopes, because of the neutron occupation of the  $2s$  orbit,  $^{24}\text{O}$  ( $N = 16$ ) provides another example to show a significant jump in  $f_{\text{PDR}}$  from  $^{22}\text{O}$  [8]. This nucleus has the strongest linear correlation with  $r = 0.97$ .

We also calculate the correlation coefficient for  $^{132}\text{Sn}$ . It indicates a relatively weak correlation with  $r = 0.68$ . Note that  $^{132}\text{Sn}$  corresponds to a kink point similar to  $^{78}\text{Ni}$  in Fig. 2. Namely, the PDR fraction in Sn isotopes will jump up beyond  $N = 82$  [18]. The correlation coefficients are summarized in the second column of Table I for various nuclei.

Let us briefly comment on the effect of the pairing and the continuum. For the effect of pairing, we compare our result with that of the canonical-basis time-dependent Hartree-Fock-Bogoliubov calculation [17,19]. The effect of the continuum is examined by enlarging  $R_{\text{box}}$  to 20 and 25 fm. We have confirmed that these effects do not affect the present conclusion. It should be worth mentioning that, in this Rapid Communication, we do not treat nuclei with a neutron separation energy smaller than 3 MeV.

*Deformed nuclei.* The deformation effect seems to somewhat weaken the correlation. Figure 4 shows two deformed nuclei,  $^{58}\text{Cr}$  with the quadrupole deformation of  $\beta_2 = 0.17$

FIG. 4. (Color online) Same as Fig. 2 but for deformed nuclei  $^{58}\text{Cr}$  and  $^{110}\text{Zr}$ . See text for details.

and  $^{110}\text{Zr}$  with a larger deformation of  $\beta_2 = 0.36$ . The  $^{58}\text{Cr}$  nucleus has the same number of neutrons as  $^{54}\text{Ca}$ , which carries a comparable PDR strength to  $^{52}\text{Ca}$  [8]. Nevertheless, the correlation in  $^{58}\text{Cr}$ ,  $r = 0.80$ , is significantly weaker than that in spherical  $^{52,54}\text{Ca}$ .  $^{110}\text{Zr}$  has an even larger deformation and a weaker correlation  $r = 0.74$ , although it has sizable PDR strength. The ground-state deformation is expected to produce a peak splitting both in the PDR and in the GDR. Due to the complicated characters in the  $E1$  strength distribution, the PDR strength  $S_{\text{PDR}}$  may be contaminated by the low-energy tail of the GDR strength.

*Universal behaviors.* The property of the linear correlation is very robust with respect to the choice of Skyrme energy functionals. In Fig. 5, we show the same correlation plot as Fig. 2 calculated with the parameter set of SkM\* replaced by SIII [20] and SGII [21]. All three Skyrme functionals yield a relatively weak correlation for  $^{68}\text{Ni}$  with  $r = 0.65\text{--}0.75$  and a strong linear correlation for  $^{84}\text{Ni}$  with  $r > 0.94$ . A strong correlation with  $r \approx 0.95$  is also confirmed for  $^{24}\text{O}$  and  $^{54}\text{Ca}$ .

The slope of the straight line, obtained by linear fit, turns out to be universal too, with respect to different Skyrme energy functionals. All these three parameter sets (SkM\*, SGII, and SIII) produce the similar slope of  $dS_{\text{PDR}}/d(\Delta r_{np}) = 13\text{--}16 e^2 \text{ fm}$  for  $^{84}\text{Ni}$ . We observe the linear correlation of  $f_{\text{PDR}}$  instead of  $S_{\text{PDR}}$  as well with respect to  $\Delta r_{np}$ . However, in this case, the slope obtained by the linear fit has a sizable dependence on the functionals.

*Correlation among different energy functionals.* Instead of slightly modifying the Skyrme parameters, we next examine the correlation that adopts many different Skyrme functionals that correspond to a variety of values of the  $L$  parameter; SIII, SGII, SkM\*, SLy4 [22], SKT4 [23], SkI2, SkI3, SkI4, SkI5 [24], UNEDF0, and UNEDF1 [25]. From these 11 different

TABLE I. Calculated correlation coefficients  $r$  between  $\Delta r_{np}$  and  $S_{\text{PDR}}$  for selected nuclei. The SkM\* parameter set is adopted for the central values. The values of variable  $\omega_c$  also are listed. Note that we cannot identify a prominent PDR peak for  $^{48}\text{Ca}$ .  $r^{(v)}$ 's are obtained with the variable cutoff energies  $\omega_c$  in the fourth row. The correlation coefficients larger than 0.9 are shown in boldface.

	$^{24}\text{O}$	$^{26}\text{Ne}$	$^{48}\text{Ca}$	$^{52}\text{Ca}$	$^{54}\text{Ca}$	$^{68}\text{Ni}$	$^{78}\text{Ni}$	$^{84}\text{Ni}$	$^{58}\text{Cr}$	$^{110}\text{Zr}$
$r$	<b>0.97</b>	0.83	0.78	<b>0.91</b>	<b>0.96</b>	0.69	0.76	<b>0.94</b>	0.80	0.74
$r^{(v)}$	<b>0.97</b>	0.88		<b>0.92</b>	<b>0.94</b>	0.77	<b>0.92</b>	<b>0.96</b>	0.80	0.84
$\omega_c$ (MeV)	8.29	9.95		10.49	9.41	11.48	8.73	8.59	9.82	8.36

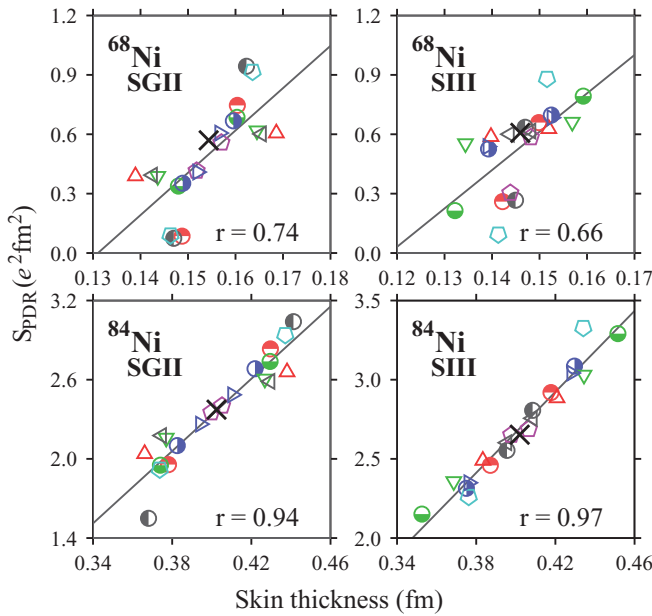


FIG. 5. (Color online) Same as Fig. 2 but for  $^{68,84}\text{Ni}$  with SGII and SIII interactions.

parameter sets, we estimate the correlation coefficient  $r$  in Eq. (3) with  $N_d = 11$ . Again, we have found a weak correlation with  $r = 0.47$  for  $^{68}\text{Ni}$  and a strong correlation  $r = 0.89$  for  $^{84}\text{Ni}$ .

We also examine the correlation between the slope parameter of the symmetry energy  $L$  and the PDR fraction  $f_{\text{PDR}}$  in  $^{68}\text{Ni}$  and  $^{84}\text{Ni}$ . This leads to the similar coefficients  $r = 0.37$  and  $0.84$  for  $^{68}\text{Ni}$  and  $^{84}\text{Ni}$ , respectively. Thus, to quantitatively constrain  $\Delta r_{np}$  and  $L$ , the measurement of the PDR in the very neutron-rich  $^{84}\text{Ni}$  is more favored than in  $^{68}\text{Ni}$ .

The small correlation coefficient between  $L$  and  $f_{\text{PDR}}$  for  $^{68}\text{Ni}$  ( $r = 0.37$ ) turns out to be due to the fact that the choice of  $\omega_c = 10$  MeV has different meanings for different functionals. Namely, the different energy functionals produce different PDR peak energies, some of which are below 10 MeV, but some are above that. The tail of the GDR strength also depends on the choice of the energy functionals. Therefore, to perform a more sensible analysis for this study, we should use the variable cutoff  $\omega_c$ . This will be discussed below.

*Use of variable  $\omega_c$ .* The PDR strength (1) and PDR fraction (2) based on variable  $\omega_c$  are, hereafter, referred to as  $S_{\text{PDR}}^{(v)}$  and  $f_{\text{PDR}}^{(v)}$ , respectively. The variable  $\omega_c$  is determined according to the following procedure: The calculated (discrete)  $B(E1)$  values are smeared with the Lorentzian with a width of  $\gamma = 1$  MeV. By plotting this smeared  $E1$  strength  $S(E1; E)$  as a function of energy, if we can find a distinguishable PDR peak and its energy  $E_{\text{peak}}$ ,  $\omega_c$  is defined as the energy that corresponds to the minimum value of  $S(E1; E)$  at  $E > E_{\text{peak}}$ . In Fig. 6, as an example, the determination of  $\omega_c$  is shown for  $^{84}\text{Ni}$ . Since the determination of the variable  $\omega_c$  requires a noticeable PDR peak structure, it is difficult to define  $S_{\text{PDR}}^{(v)}$  for most of the stable isotopes.

The values of  $\omega_c$  vary from nucleus to nucleus within a range of  $10 \pm 2$  MeV for those listed in Table I. Note that

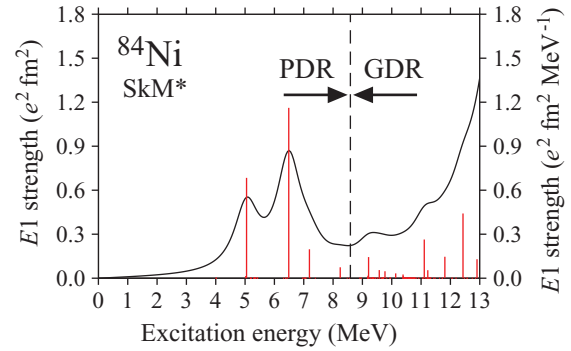


FIG. 6. (Color online) Calculated  $E1$  strengths [ $B(E1; n)$ , vertical lines] for  $^{84}\text{Ni}$  in units of  $e^2 \text{fm}^2$  and those smeared with the width of  $\gamma = 1$  MeV [ $S(E1; E)$ , solid curve] in units of  $e^2 \text{fm}^2 \text{MeV}^{-1}$ . According to the procedure described in the text, the cutoff energy is determined as  $\omega_c = 8.59$  MeV.

$\omega_c$  may also change when we slightly modify the Skyrme parameters. Although the correlation is slightly enhanced by replacing  $S_{\text{PDR}}$  with  $S_{\text{PDR}}^{(v)}$  in most cases, they are approximately similar,  $r^{(v)} \approx r$ . In Table I, there are a few exceptions;  $^{78}\text{Ni}$  ( $r = 0.76 \rightarrow r^{(v)} = 0.92$ ),  $^{68}\text{Ni}$  ( $r = 0.69 \rightarrow r^{(v)} = 0.77$ ), and deformed  $^{110}\text{Zr}$  ( $r = 0.74 \rightarrow r^{(v)} = 0.84$ ). In these cases, we found that the separation between PDR and GDR is somewhat ambiguous, and the results depend on the choice of  $\omega_c$ . On the other hand, isotopes that indicate  $r > 0.9$  with fixed  $\omega_c = 10$  MeV show  $r^{(v)} \approx 1$  with the variable  $\omega_c$  as well. In Ni isotopes, although the values of  $r^{(v)}$  are slightly different from  $r$ , it is confirmed that the linear correlation is significantly stronger in  $^{84}\text{Ni}$  than in  $^{68}\text{Ni}$ .

For eleven different parameter sets, the correlation between  $S_{\text{PDR}}^{(v)}$  and  $\Delta r_{np}$  for  $^{68,84}\text{Ni}$  is shown in the upper part of Fig. 7. A strong positive correlation ( $r^{(v)} > 0.9$ ) between PDR strength

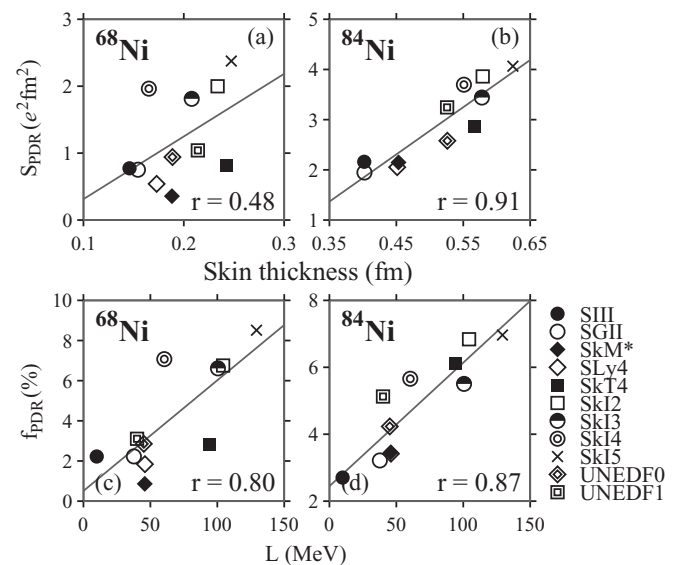


FIG. 7. Correlations between  $S_{\text{PDR}}^{(v)}$  and  $\Delta r_{np}$  (top panels), and between  $f_{\text{PDR}}^{(v)}$  and  $L$  (bottom panels) for  $^{68}\text{Ni}$  (left) and  $^{84}\text{Ni}$  (right), among 11 different Skyrme functionals.

$S_{\text{PDR}}^{(v)}$  and  $\Delta r_{np}$  can be seen in  $^{84}\text{Ni}$ . In contrast, it is significantly weaker for  $^{68}\text{Ni}$  ( $r^{(v)} = 0.48$ ). The bottom part of Fig. 7 shows the correlation between  $f_{\text{PDR}}^{(v)}$  and slope parameter  $L$  of the symmetry energy. Again, the correlation is stronger for  $^{84}\text{Ni}$  with  $r^{(v)} = 0.87$  than  $^{68}\text{Ni}$  with  $r^{(v)} = 0.80$ . The correlation between  $\Delta r_{np}$  and  $L$  has a similar trend,  $r^{(v)} = 0.88$  for  $^{84}\text{Ni}$  and  $r^{(v)} = 0.84$  for  $^{68}\text{Ni}$ . Basic features of the correlation with the variable  $\omega_c$  are consistent with those obtained with  $\omega_c$  fixed at 10 MeV. Thus, the PDR strength in  $^{84}\text{Ni}$  with many excess neutrons can provide a better constraint on  $L$  and the neutron skin compared to  $^{68}\text{Ni}$ .

*Summary.* We have studied the correlation of the PDR and the neutron-skin thickness for nuclei with  $Z \leq 40$  and  $^{132}\text{Sn}$ . We have found that a strong linear correlation is seen only in particular nuclei. The PDR strength has a very strong linear correlation with the neutron-skin thickness in spherical neutron-rich nuclei with  $14 < N \leq 16$ ,  $28 < N \leq 34$ , and  $50 < N \leq 56$ . In these regions, the neutron Fermi levels are located at the loosely bound low- $\ell$  shells, and the PDR strengths significantly increase as the neutron numbers increase. Nuclei

outside of these regions have weaker correlations. This linear correlation is robust with respect to the choice of the energy functional parameter set. This suggests that the experimental observation of PDR in properly selected neutron-rich nuclei could be a possible probe of the neutron-skin thickness  $\Delta r_{np}$  and a constraint on the slope parameter  $L$  of the symmetry energy. The linear correlation seems to be weakened by the deformation due to the peak splitting of the PDR and the GDR. The present result may provide a solution for the controversial issue on the correlation between the PDR and the neutron skin for which different conclusions previously were reported [3,4,6,26].

This work was partly supported by HPCI System Research Projects (Projects No. hp120192 and No. hp120287), by PACS-CS project (Projects No. 13a-33, No. 12a-20, and No. 11a-21), and by JSPS KAKENHI Grants No. 21340073, No. 24105006, No. 25287065, and No. 25287066. The numerical calculations were partially performed on the RIKEN Super Combined Cluster (RSCC).

- 
- [1] B. A. Brown, *Phys. Rev. Lett.* **85**, 5296 (2000).
  - [2] R. J. Furnstahl, *Nucl. Phys. A* **706**, 85 (2002).
  - [3] J. Piekarewicz, *Phys. Rev. C* **73**, 044325 (2006).
  - [4] A. Klimkiewicz *et al.*, *Phys. Rev. C* **76**, 051603(R) (2007).
  - [5] A. Carbone *et al.*, *Phys. Rev. C* **81**, 041301(R) (2010).
  - [6] P.-G. Reinhard and W. Nazarewicz, *Phys. Rev. C* **81**, 051303(R) (2010).
  - [7] P.-G. Reinhard and W. Nazarewicz, *Phys. Rev. C* **87**, 014324 (2013).
  - [8] T. Inakura, T. Nakatsukasa, and K. Yabana, *Phys. Rev. C* **84**, 021302(R) (2011).
  - [9] T. Nakatsukasa, T. Inakura, and K. Yabana, *Phys. Rev. C* **76**, 024318 (2007).
  - [10] T. Inakura, T. Nakatsukasa, and K. Yabana, *Phys. Rev. C* **80**, 044301 (2009).
  - [11] P. Avogadro and T. Nakatsukasa, *Phys. Rev. C* **84**, 014314 (2011).
  - [12] M. Stoitsov, M. Kortelainen, T. Nakatsukasa, C. Losa, and W. Nazarewicz, *Phys. Rev. C* **84**, 041305(R) (2011).
  - [13] P. Avogadro and T. Nakatsukasa, *Phys. Rev. C* **87**, 014331 (2013).
  - [14] T. Inakura *et al.*, *Nucl. Phys. A* **768**, 61 (2006).
  - [15] T. Nakatsukasa and K. Yabana, *Phys. Rev. C* **71**, 024301 (2005).
  - [16] J. Bartel, P. Quentin, M. Brack, C. Guet, and H. B. Håkansson, *Nucl. Phys. A* **386**, 79 (1982).
  - [17] S. Ebata *et al.*, *Phys. Rev. C* **82**, 034306 (2010).
  - [18] S. Ebata, T. Nakatsukasa, and T. Inakura, [arXiv:1201.3462](https://arxiv.org/abs/1201.3462);
  - [19] S. Ebata (private communication).
  - [20] M. Beiner, H. Flocard, N. van Giai, and P. Quentin, *Nucl. Phys. A* **238**, 29 (1975).
  - [21] N. Van Giai, and H. Sagawa, *Phys. Lett. B* **106**, 379 (1981).
  - [22] E. Chabanat, P. Bonche, P. Haensel, J. Mayer, and R. Schaeffer, *Nucl. Phys. A* **627**, 231 (1998).
  - [23] F. Tondeur, M. Brack, M. Farine, and J. M. Pearson, *Nucl. Phys. A* **420**, 297 (1984).
  - [24] P.-G. Reinhard and H. Flocard, *Nucl. Phys. A* **584**, 467 (1995).
  - [25] M. Kortelainen *et al.*, *Phys. Rev. C* **85**, 024304 (2012).
  - [26] S. Volz *et al.*, *Nucl. Phys. A* **779**, 1 (2006).